

Finite Element Modeling of Reinforced Concrete Beams Under Static Loading Using Abaqus Software

Sai Pavan Bandaru

PG student, Department of Civil Engineering, QIS college of Engineering and Technology, Ongole, Vengamukkapalem, Andhra Pradesh 523272.

Anjaneyulu G, Kalyani Gurram, Maheswararao R and Venugopal P

Assistant professor, Department of Civil Engineering, QIS college of Engineering and Technology, Ongole, Vengamukkapalem, Andhra Pradesh 523272.

Corresponding Author: Sai Pavan Bandaru

Published online: May 2026

DOI Link: <https://doi.org/10.64971/j.cph.eijtem.v13.i2.22.2026>

Abstract:

The flexural behavior of reinforced concrete (RC) beams is examined in this work in relation to concrete strength and reinforcement details. Under two-point loads, uniform-sized beam specimens with concrete grades M25, M30, and M40 and reinforcement ratios ranging from 0.50% to 1.28% were tested. According to the findings, M25, M30, and M40 had 28-day compressive strengths of 27.6 MPa, 32.8 MPa, and 43.2 MPa, respectively, indicating a 56% improvement in material stiffness and quality. Performance testing showed that when reinforcement ratios increased, the ultimate loads increased from 55.0 kN to 75.0 kN and the first fracture load increased from 16.5 kN for M25 to 22.5 kN for M40. Furthermore, the mid-span deflection decreased from 11.2 mm to 7.6 mm. Beams with higher reinforcement showed multiple finer cracks, which are a sign of enhanced ductility, while those with lesser reinforcement showed fewer but wider fissures. The dependability of the FEM model was confirmed by finite element analysis (FEM) using ABAQUS, which supported the experimental results with a variation of 2% to 5% between FEM and experimental data. Fracture initiation patterns were consistent with flexural theory, and stress contours showed the anticipated compression and tension distributions. Overall, the results show that while concrete grade is still essential for stiffness and fracture resistance, higher reinforcing percentage improves load capacity and ductility, greatly impacting structural performance. It is advised to use the verified FEM model as a useful tool for predicting RC behavior and optimizing structural design.

Keywords:

Concrete Grade, Reinforcement Ratio, ABAQUS, Finite Element Analysis, Concrete Damaged Plasticity.

1. Introduction

FEA is a widely used computational technique for modeling the structural behavior of RC beams under both static and dynamic stresses. A thorough assessment of nonlinear material properties, crack formation, and load-deflection responses all of which are frequently difficult to characterize analytically is made possible by FEA. The intricate stress interactions in RC structures made of steel and concrete composites can be precisely predicted by a well-calibrated FEA model. In 3D nonlinear simulations, the complex Concrete Damaged Plasticity (CDP) model in ABAQUS, a popular FEA package, efficiently captures critical phenomena such cracking, stiffness deterioration, and crushing. When it comes to shifting loads from slabs to columns and foundations, RC beams are essential. Because of the interaction between steel and concrete, their structural performance is complicated, displaying a variety of behavior stages, including elastic response before to cracking, crack initiation from tensile stresses, stiffness loss following cracking, yielding of reinforcement, and eventual failure. In order to guarantee structural safety, serviceability, and economic considerations, it is essential to comprehend and anticipate these behaviors.

The conventional dependence on analytical techniques based on classical theory, which frequently assume linear material behavior and idealized stress distribution, highlights the necessity of finite

element modeling of RC beams. These analytical models are insufficient because RC displays strong nonlinear characteristics as a result of several failure mechanisms. By enabling the discretization of structures into smaller, more manageable elements that accurately represent geometrical and material nonlinearities, FEA overcomes these limitations and makes it possible to predict load-deflection behavior, crack initiation and propagation, stress distribution, and failure modes. High specimen preparation expenses, time-consuming testing, a narrow field of parameter analysis, and difficulties in monitoring internal stress states are some of the limitations of conventional analytical methods. Although experimental testing advances our knowledge of the behavior of RC beams, it does not always offer comprehensive details regarding the formation of cracks or the deterioration of stiffness. By minimizing reliance on lengthy laboratory experiments and enhancing experimental investigations, FEA provides a solution.

Among the general-purpose finite element programs used in civil engineering research, ABAQUS is particularly useful for nonlinear structural analysis. It has strong constitutive models for concrete, the most prominent of which is the CDP model. Tensile cracking, compressive crushing, damage-induced stiffness deterioration, and plastic deformation reactions under increasing pressures are all simulated by this model. Additionally, ABAQUS improves simulations of composite activities between concrete and steel by ensuring precise modeling of reinforcement through embedded restrictions. Concrete mix proportions have a major impact on mechanical properties including modulus of elasticity, tensile strength, and compressive strength. The stiffness and load-bearing capability of reinforced concrete beams can be impacted by even small changes in the water-to-cement ratio, cement quantity, and aggregate distribution. Many studies ignore these differences in favor of typical material attributes, which can distort assessments of the performance of RC beams. While more cement can improve bonding, changes in mix proportions, such as a lower water-to-cement ratio, typically increase strength and decrease permeability. Therefore, correct evaluations of the structural behavior of concrete in real-world applications depend on the incorporation of genuine material attributes indicative of the mix design.

For many years, researchers have studied RC beams respond to static loads, concentrating on load-deflection response, failure mechanisms, and cracking behavior. Although instructive, traditional experimental approaches are expensive and time-consuming, which has led to a trend toward computational techniques like the FEM. Because of its complex CDP model and dependable nonlinear solvers, ABAQUS has become a crucial numerical tool. This chapter examines earlier computational and experimental research on the static behavior of RC beams, focusing on problems like crack growth and stiffness deterioration.

Park and Paulay's (1975) discoveries into nonlinear behavior and the effect of cracking on stiffness, which were further reinforced by Kwak and Filippou (1990), are examples of early research that established fundamental knowledge [1,14]. They emphasized that cracking dramatically lowers post-elastic stiffness, which is important for numerical modeling. The significance of concrete strength and reinforcing details on load characteristics has been validated by more recent research.

Discretizing the structure and employing nonlinear material models to capture cracking and crushing are key components of FEM's ability to accurately represent the behavior of RC beams. These techniques were developed by researchers such as Ngo and Scordelis (1967) and later improved by Vecchio and Collins (1986) with the Modified Compression Field Theory [9-10]. The CDP model was created by Lubliner et al. (1989) and Lee and Fenves (1998), demonstrating its usefulness in simulating RC beams under static loads [12-13]. It is well-known for its ability to simulate cracking and damage (Hanif et al., 2018; Pazdan, 2021) [16-17].

In FEM, accurate modeling of reinforcement is essential, usually utilizing truss or beam elements in conjunction with concrete solid elements. This is made easier by ABAQUS's embedded region technique, albeit it frequently presumes a perfect link between materials. FEM accuracy is strongly influenced by mesh size and element type; C3D8R elements are suggested to balance computational needs and precision. There aren't many research on mesh sensitivity, though.

It is essential to validate the model against experimental results. For example, Abdullah et al. (2024) found that when comparing ABAQUS models with experimental data, prediction errors for ultimate loads ranged from 5% to 10%. Flexural performance may be consistently predicted using FEM if material parameters are adequately described, according to research on RC beams manufactured from recycled aggregates. In addition to emphasizing the mutually beneficial interaction between experimental and computational methods in expanding our understanding of RC beam behavior, this requirement for numerical simulations highlights the limitations of experimental investigations due to resource restrictions [18].

With an emphasis on various concrete grades (M25, M30, and M40) affect strength, stiffness, and cracking, the study attempts to examine the flexural response of reinforced concrete beams under

two-point loading. It will establish important structural characteristics like deflection, crack patterns, and load thresholds, as well as evaluate the effects of tensile reinforcement percentages (0.50% to 1.28%) on ductility and load capacity. The research entails assessing compressive strength at 7 and 28 days, examining load-deflection behavior, and developing an ABAQUS finite element model to replicate the behavior of RC beams. The interaction between steel and concrete will be simulated using the Concrete Damaged Plasticity model for nonlinear behavior description. Finally, it will assess the accuracy of the analysis and draw conclusions for optimizing the design of reinforced concrete beams by comparing experimental and FEM data.

2. Materials & Methods

The quality and suitability of the materials employed are crucial to the performance of reinforced concrete beams. The materials used in this part were chosen in accordance with Indian Standards for repeatability and uniformity.

2.1 Cement

Ordinary Portland Cement (43 grade) was selected because it provides adequate setting times and strength development, making it suitable for structural applications. Physical characteristics, such as a specific gravity of 3.15, an initial setting time of 38 minutes, a final setting time of 510 minutes, and a 28-day compressive strength of 44.8 MPa, verify compliance with IS 8112:2013.

2.2 Fine Aggregate

To guarantee workability and low void content in the concrete, natural river sand with a Zone II grading was used. It has a water absorption rate of 1.1%, a fineness modulus of 2.71, and a specific gravity of 2.64.

2.3 Coarse aggregates

The concrete's compressive strength and stiffness were greatly impacted by the use of crushed granite aggregate with a maximum size of 20 mm, which was chosen for its impact resistance. With a water absorption of 0.5% and an aggregate impact value of 19.6%, the specific gravity is 2.68.

2.4 Steel reinforcement

For both longitudinal and transverse reinforcement, high yield strength deformed steel bars of Fe 500 grade were used, improving ductility and load-carrying capacity. With an elongation percentage of 14.5%, the modulus of elasticity is 200 GPa, the yield strength is 500 MPa, and the ultimate strength is 620 MPa.

Two bars with a diameter of 10 mm for top compression and 8 mm stirrups spaced 150 mm apart for shear reinforcement were used in the reinforcement configuration to guarantee beam flexural failure. Tensile steel was tested at different percentages; the specifics are as follows: B5 contained high steel (1.28%), B3 and B4 were control specimens with 0.72%, and B1 and B2 had low steel (0.50%).

2.5 Casting and curing

In this study, concrete mix design was conducted according to IS 10262:2019 to achieve the necessary strength and workability for various concrete grades. Three grades M25, M30, and M40 were used to examine the effect of concrete strength on the flexural behavior of reinforced concrete beams. The final mix proportions were established considering workability, aggregate characteristics, and water-to-cement ratio.

Key parameters for the mix design included: OPC 43 Grade as the type of cement, a maximum aggregate size of 20 mm, Zone II river sand as the fine aggregate, a medium degree of workability with a slump of 75-100 mm, moderate exposure conditions, and vibration as the method of compaction.

Table 1 Concrete Mix Proportion for different Grades

Grade	Water-Cement Ratio	Cement (kg/m ³)	Fine Aggregate (kg/m ³)	Coarse Aggregate (kg/m ³)	Water (kg/m ³)
M25	0.50	340	720	1150	170
M30	0.45	380	690	1120	171
M40	0.40	420	650	1100	168

The beam specimens were designed as under-reinforced sections to ensure flexural failure occurred prior to shear failure. They were simply supported and subjected to two-point loading, creating a constant moment region at mid-span. The geometry and reinforcement detailing were standardized to ensure consistent results attributed to material behavior rather than geometric variations.



Figure 1 Casting and curing of RC beams

Table 2 Details of Beam Specimens

Specimen	Concrete Grade	Bottom Reinforcement	% Steel	Variation
B1	M25	2-10 mm	0.50%	Low grade + low steel
B2	M30	2-10 mm	0.50%	Medium grade
B3	M30	2-12 mm	0.72%	Control specimen
B4	M40	2-12 mm	0.72%	Higher grade
B5	M40	2-16 mm	1.28%	High grade + high steel

Concrete was mixed mechanically for uniformity and placed in layers compacted with a needle vibrator to remove air. After demoulding at 24 hours, the specimens underwent water curing for 28 days, promoting complete hydration and enhanced strength development.

2.6 Test program

A loading frame was used to test the beams under static loading. LVDTs positioned at mid-span were used to measure deflections when the load was introduced gradually in equal stages. At each increase in load, the development and spread of cracks were visually seen and noted. Testing went on until it failed.

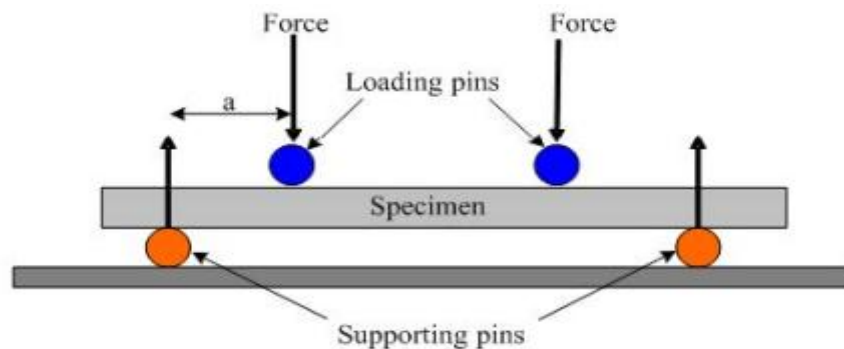


Figure 2. Four-point flexure test

3. FEM modelling in abaqus

The nonlinear response of reinforced concrete beams under static stresses was modeled using finite element analysis using ABAQUS. Stress distribution, fracture initiation, and post-cracking behaviour all of which are challenging to observe through experimental alone can be thoroughly investigated using this numerical approach. To account for variations in stiffness and strength, different concrete classes (M25, M30, and M40) were given the required elastic qualities.

3.1 Procedure for modelling

The first step in the modeling process for reinforced concrete beams is to define the beam's geometry in the Part module as a 3D deformable solid. The beam's precise dimensions 1500 mm in length, 150 mm in width, and 250 mm in depth ensure precise geometry to affect stress distribution. Stirrups and longitudinal bars are examples of reinforcement bars that are made independently to meet design-specific spacing requirements.

Table 3 Element Types Used in ABAQUS

Component	Element Type	Description
Concrete	C3D8R	8-node solid reduced integration
Reinforcement	T3D2	2-node truss element
Support Plates	R3D4	Rigid body elements

The Property module defines the constitutive models for materials, simulating tensile cracking and compressive failure using the CDP model. To fit experimental results, parameters are chosen from the literature and represented by different ABAQUS element types, such as T3D2 for reinforcement and C3D8R for concrete.

Table 4 Concrete Damage Plasticity (CDP) Parameters

Parameter	Value
Dilation Angle (°)	36
Flow Potential Eccentricity	0.1
fb0 / fc0	1.16
K	0.67
Viscosity Parameter	0.0005

Table 5 Elastic Properties of Materials in FEM

Concrete Grade	Compressive Strength (fck) (MPa)	Modulus of Elasticity (Ec) (GPa)	Poisson's Ratio
M25	25	25.0	0.20
M30	30	27.4	0.20
M40	40	31.6	0.20

A perfect link between steel and concrete is assumed, and steel reinforcement is described as an elastic-plastic material with isotropic hardening properties.

While truss sections show the bar diameter of the reinforcement, sections are given post-material definition to guarantee correct correlation of the concrete beam with the solid section. For correct physical representations in modeling, this phase is essential.

In order to prevent inaccurate results, the Assembly module addresses spacing and alignment in addition to proper beam and reinforcing bar positioning and centering. By defining connections between concrete and reinforcement under the assumption of perfect bonding and no slippage, the embedded region interaction technique preserves structural model fidelity.

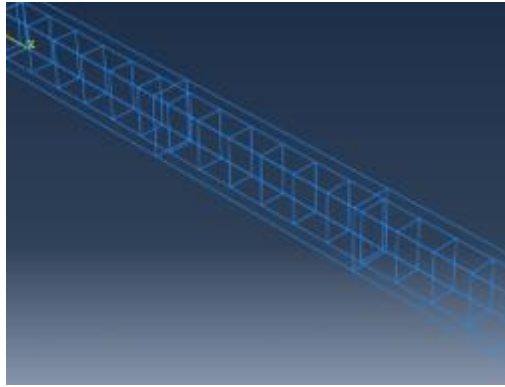


Figure 3 Assembly of the Elements

A Static General method is used to simulate the analysis phase, which permits large deformations and nonlinear behavior. Boundary conditions are used to control vertical movements at supports and simulate simply supported conditions. Two-point vertical displacements are used to produce loading.

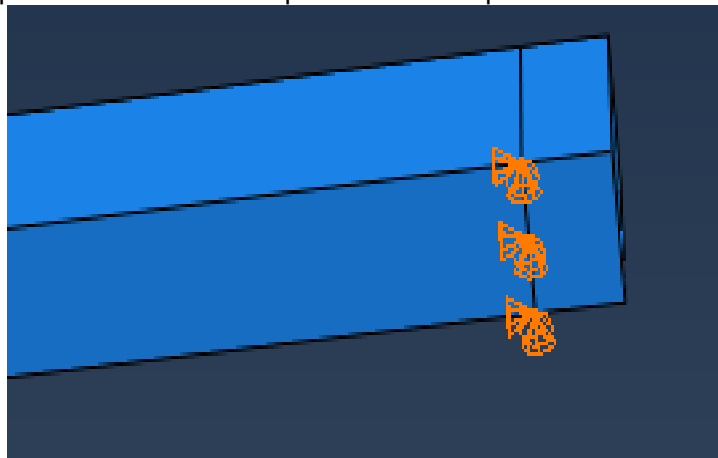


Figure 4 Points Loads and Bottom Supports
Table 6 Boundary Conditions and Loading

Location	Constraint
Left Support	$U_x = U_y = U_z = 0$
Right Support	$U_y = U_z = 0$
Load Application	Two-point vertical displacement

Performance is guided by mesh refinement studies, which determine that a mesh size of 25 mm strikes a compromise between computing efficiency and result accuracy.

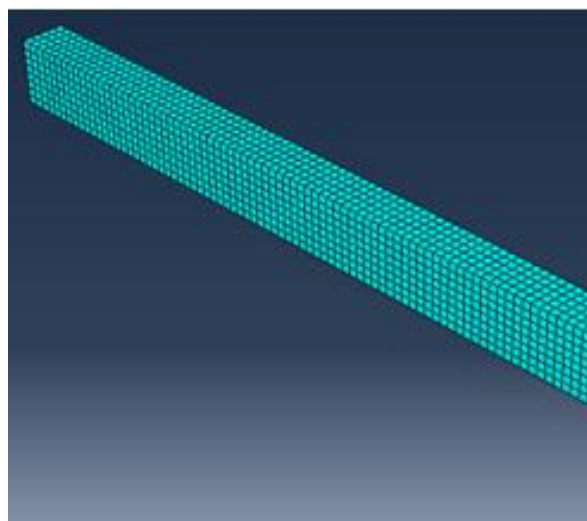


Figure 5 Meshing of RC Beam

In the last stage, a simulation execution job is created, in which ABAQUS iteratively solves equations while monitoring convergence and modifying load increments. Load-deflection graphs and stress patterns that show damage to steel and concrete are among the results.

4. Results and discussion

Results from FEM and experimental testing of reinforced concrete beams are presented in this chapter. Compressive strength using the cube test, load-deflection response, start and terminal crack loads, fracture patterns, and modes of failure are important evaluations that are validated by FEM data. The effects of concrete grades (M25, M30, M40) and steel percentage (0.50%-1.28%) are examined numerically.

4.1 Compressive strength

The results show that, for all grades, concrete's compressive strength increases with curing time. Concrete usually reaches 65-70% of its strength after 7 days; M25 reaches 18.2 MPa after 7 days and 27.6 MPa after 28 days. By 28 days, all grades surpass their characteristic strengths: M25 reaches 27.6 MPa (10.4% above target), while M30 and M40 reach 32.8 MPa and 43.2 MPa, respectively, exceeding targets by 9.3% and 8%. Because of better particle packing and lower water-cement ratios, the strength increases by 56% from M25 to M40. The enhanced stiffness, decreased deflection, and improved fracture resistance that come from M40's higher compressive strength improve beam performance and increase the load-bearing capacity of the compression zone.

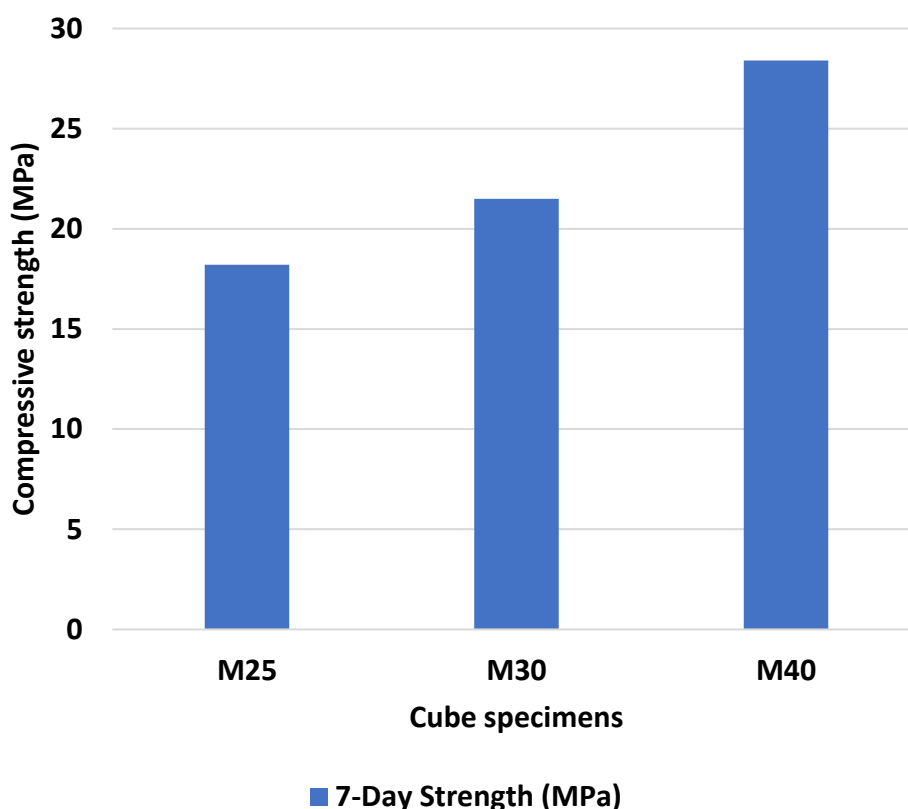


Figure 6 Compressive strength of cube samples

4.2 Load-Deflection of RC beams

The linear elastic stage, the cracking stage, and the nonlinear post-cracking stage are the three phases of load-deflection response in reinforced concrete beams under flexural loading. Beams first show linear behavior when steel and concrete withstand stresses up to 16.5-22.5 kN. Compared to M25, higher-grade concrete (M40) offers more rigidity. Microcracks start the cracking stage, with specimens B5 and B1 exhibiting decreased tensile resistance at 22.5 kN and 16.5 kN, respectively. Because broken concrete contributes less tensile force, stiffness decreases. With maximum deflections of 11.2 mm for B1 and 7.6 mm for B5, the post-cracking stage exhibits nonlinear behavior and a 32% decrease associated with higher concrete grade. Results using the FEM show reduced deflections of 7.0 mm for B5 and 10.5 mm for B1, supporting experimental data and demonstrating the predicted accuracy of the model.

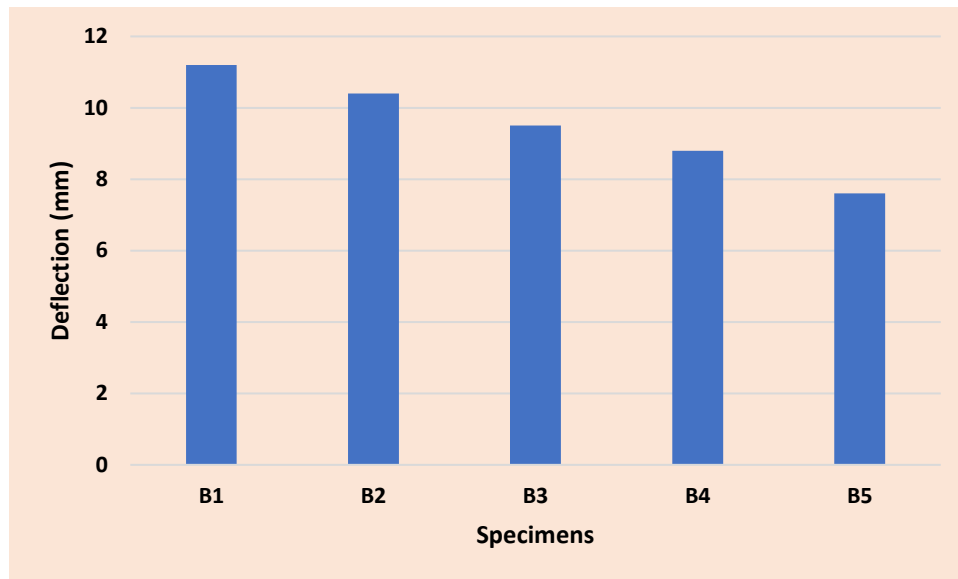


Figure 7 Deflections of all sample specimens

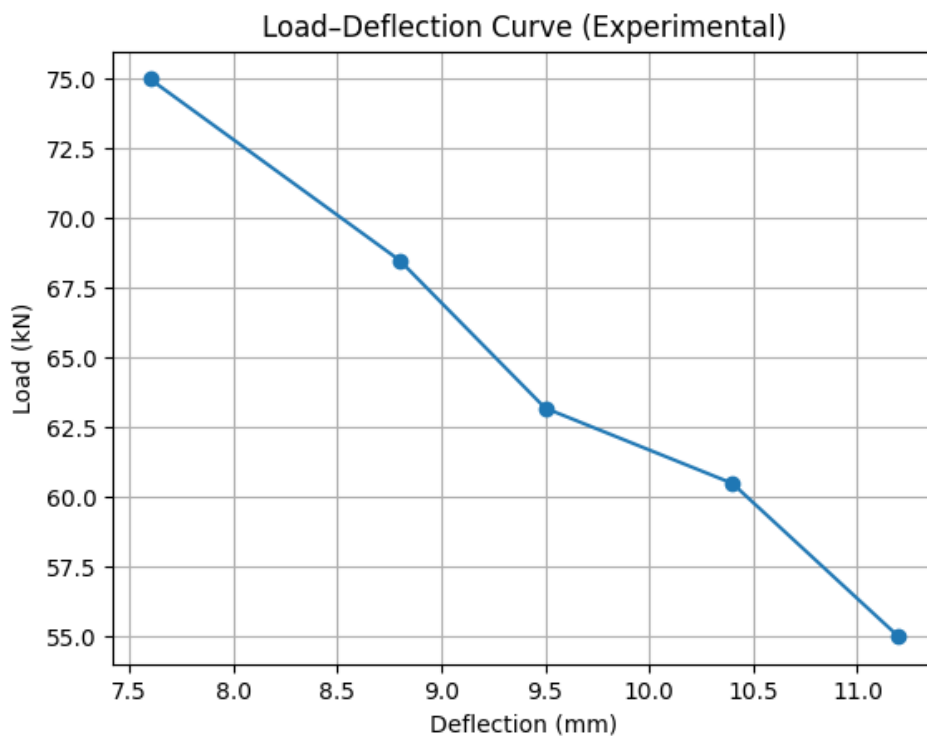


Figure 8 Load-Deflection Curve of RC beams

4.3 Discussion on first crack & Ultimate load capacity

For determining the tensile strength of concrete, the first crack load—which indicates the transition from elastic behavior to cracking is essential. Tensile strength is shown to improve from 16.5 kN in B1 (M25) to 22.5 kN in B5 (M40), a 36% increase associated with higher concrete grades and reinforcing ratios. With minor differences because of model assumptions, FEM analysis predicts fracture loads of 17.0 kN for B1 and 23.5 kN for B5. The ultimate load capacity increases steadily, from 55.0 kN for B1 to 75.0 kN for B5, by about 36.4%. This rise is mostly due to the steel percentage, which increases tensile resistance after cracking. Higher steel composition can increase strength, but if it is overreinforced, ductility may be compromised. The FEM estimates for ultimate load (57.5 kN for B1 and 78.0 kN for B5) matched the ABAQUS model, showing its accuracy in forecasting ultimate strength, and all examined beams behaved as under-reinforced sections, guaranteeing ductile failure with observable warning signals.

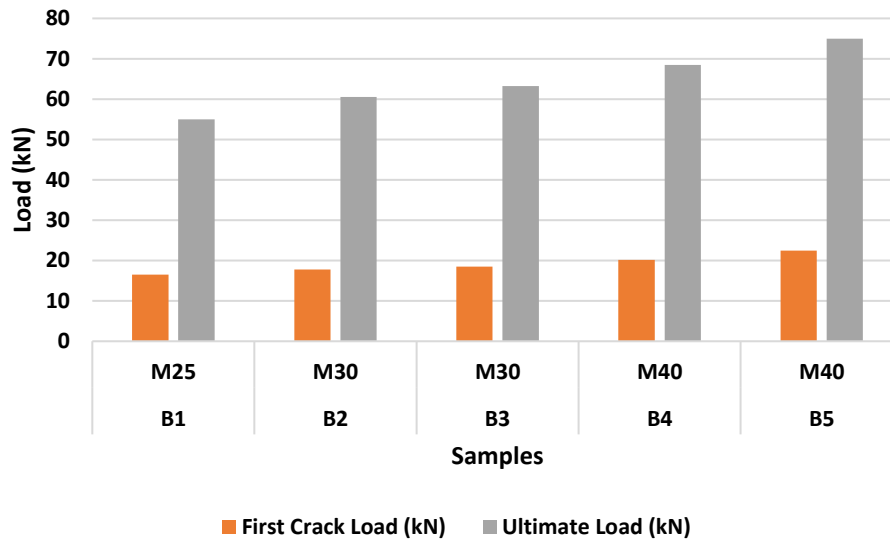


Figure 9 Specimens Vs First crack and Ultimate loads



Figure 10 Testing of RC beams

4.4 Crack pattern

Beam crack patterns provide information about the behavior and failure of the structure, especially near the mid-span when bending forces are at their highest. Higher-grade beams, like B5, display delayed, narrower cracks, indicating better crack control, whereas lower-grade beams, like B1, display faster, broader cracks due to reduced tensile strength. There is a relationship between the percentage of reinforcement and the number of cracks; longer-lasting beams with more steel have smaller, more frequent cracks. The efficiency of the CDP model in reproducing cracking behavior is validated by FEM results, which also support the bottom-up progression of tensile damage.

4.5 FEM Results using ABAQUS software

The flexural behavior of RC beams was simulated using the FEM in ABAQUS software, which included CDP for concrete and elastic-plastic behavior for steel. The approach successfully predicted important characteristics, including initial fracture load, maximum load capacity, load-deflection response, stress distribution, and crack patterns, by simulating an experimental setup under two-point loading circumstances.

Experimental findings were used to validate the nonlinear behavior, which demonstrated linear behavior up until the first crack, after which rigidity declined. Higher concrete grades and reinforcement percentages caused the deflections to rise significantly; specimens B1 and B5 had maximum deflections of 10.5 mm and 7.0 mm, respectively. Despite slightly underestimating experimental deflections, FEM calculations demonstrated a nonlinear load-deflection relationship. Higher concrete grades increased the first fracture loads by 38%, from 17.0 kN for B1 to 23.5 kN for B5, while the final load capacities increased by 35.6%, from 57.5 kN to 78.0 kN, highlighting the importance of reinforcing in improving tensile strength and load capacity.

Higher-grade concrete promotes an even stress distribution to prevent early cracking, while stress contour graphs showed concentrated compressive loads on top fibers and tensile stresses below.

Higher-reinforcement specimens had many fine cracks, while lower-reinforcement specimens had fewer but broader fissures, according to crack patterns. This finding supported the CDP model's ability to accurately replicate crack behavior. Flexural theory was supported by deformation forms, which showed maximum deflection at mid-span and decreased with higher concrete grades and reinforcing levels. However, because the model parameters were simplified, the deflection was still overestimated.

Table 7 FEM Results

Specimen	Concrete Grade	% Steel	First Crack Load (kN)	Ultimate Load (kN)	Max Deflection (mm)
B1	M25	0.50%	17.0	57.5	10.5
B2	M30	0.50%	18.5	62.0	9.8
B3	M30	0.72%	19.0	65.0	8.9
B4	M40	0.72%	21.0	70.0	8.2
B5	M40	1.28%	23.5	78.0	7.0

4.6 Comparison of Experimental and FEM Results

The results of the FEM and the experimental data show good agreement, with variances usually falling between 2% and 5%, which is considered excellent for structural engineering standards. A number of reasons might cause minor variations, including the ideal conditions assumed in FEM, such as perfect bonding, uniform material characteristics, and the lack of flaws, as well as experimental uncertainties related to measurement errors, curing conditions, and material variability. However, important features of the performance of the RC beam, such as the ultimate load, failure modes, load-deflection response, and crack formation, were well captured by the FEM technique. Additionally, the results confirm that the behavior of RC beams may be accurately simulated by the ABAQUS model, especially when CDP parameters are applied.

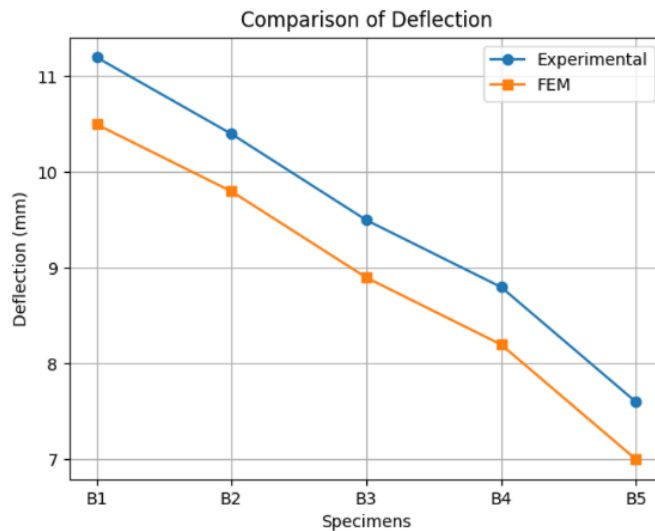


Figure 11 Comparison of Deflection (Experimental vs FEM)

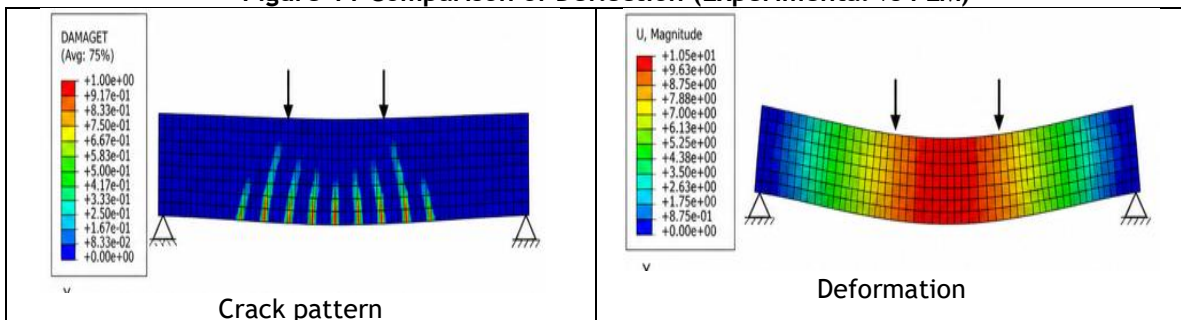


Figure 12 RC beams Crack pattern and deformation in abaqus

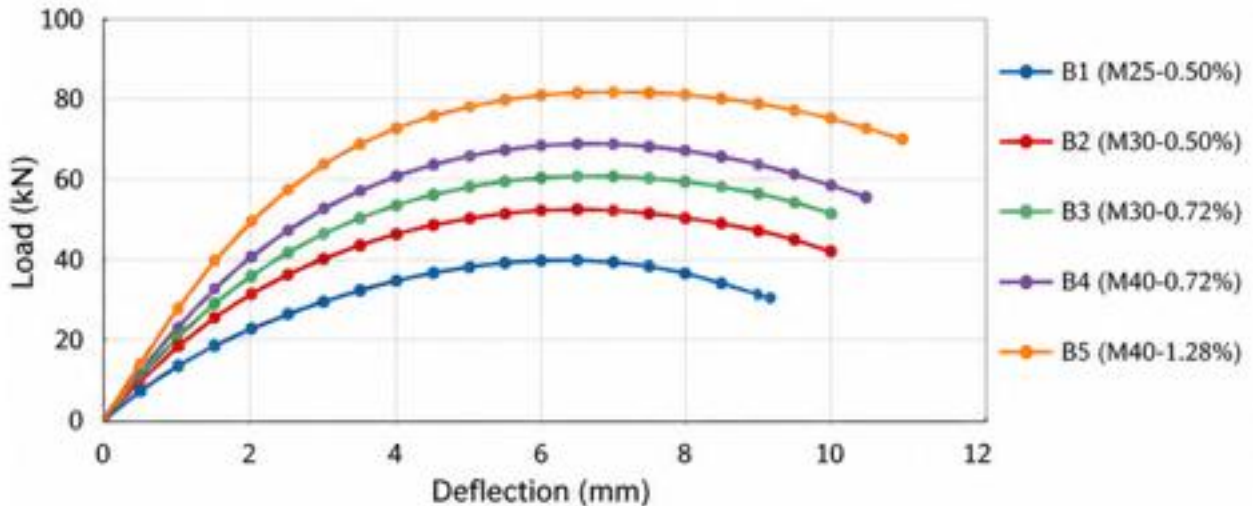


Figure 13 Load-deflection of RC beams in FEM

5. Conclusions

Using several concrete grades (M25, M30, and M40) and tensile reinforcement percentages (0.50%-1.28%), the study concentrated on the experimental and computational examination of reinforced concrete beams. It investigated the behavior of beams under flexural loads and used FEM (ABAQUS) to validate the results.

In three structural stages nonlinear post-cracking, cracking, and linear elastic reinforced concrete beams subjected to two-point loading displayed normal flexural behavior. All beams eventually broke in flexure, suggesting ductile nature, and the cracking started close to the mid-span. With a 36% increase in fracture load, smaller crack widths, and a lower maximum deflection, raising the concrete grade from M25 to M40 greatly enhanced performance while having no effect on ultimate load. The ultimate load capacity increased by 36.4% and the crack distribution improved significantly when the steel reinforcement was increased from 0.50% to 1.28%. Up until the first breaking, load-deflection responses were linear; lesser deflection was produced by higher grades and steel percentages. While ductile flexural failure was constant across specimens, cracks developed in the tension zone and showed bigger diameters with reduced steel content. The effectiveness of FEM modeling for forecasting the behavior of concrete beams was confirmed by the results, which showed a slight difference in ultimate load values and were in good agreement with testing results. In general, steel % increases ductility and load capacity, whereas concrete grade increases stiffness and durability.

References:

- Park, R., & Paulay, T. (1975). *Reinforced concrete structures*. John Wiley & Sons.
- Neville, A. M. (2011). *Properties of concrete* (5th ed.). Pearson Education.
- IS 456:2000. (2000). *Plain and reinforced concrete - Code of practice*. Bureau of Indian Standards, New Delhi.
- Kumar, R., & Bansal, P. (2018). Behavior of reinforced concrete beams under static loading. *International Journal of Civil Engineering and Technology*, 9(4), 1020-1028.
- Bathe, K. J. (2006). *Finite element procedures*. Prentice Hall.
- Zienkiewicz, O. C., Taylor, R. L., & Zhu, J. Z. (2013). *The finite element method: Its basis and fundamentals* (7th ed.). Elsevier.
- ABAQUS Documentation. (2022). *ABAQUS analysis user's manual*. Dassault Systèmes.
- Nilson, A. H., Darwin, D., & Dolan, C. W. (2010). *Design of concrete structures* (14th ed.). McGraw-Hill.
- Ngo, D., & Scordelis, A. C. (1967). Finite element analysis of reinforced concrete beams. *ACI Journal*, 64(3), 152-163.
- Vecchio, F. J., & Collins, M. P. (1986). The modified compression-field theory for reinforced concrete elements subjected to shear. *ACI Journal*, 83(2), 219-231.
- Maciej Pazdan, "FEM Modelling of Static Behaviour of RC Beams considering Nonlinear Concrete Behaviour," *Studia Geotechnica et Mechanica*, 2021.
- Lublinter, J., Oliver, J., Oller, S., & Oñate, E. (1989). A plastic-damage model for concrete. *International Journal of Solids and Structures*, 25(3), 299-326. [https://doi.org/10.1016/0020-7683\(89\)90050-4](https://doi.org/10.1016/0020-7683(89)90050-4)
- Lee, J., & Fenves, G. L. (1998). Plastic-damage model for cyclic loading of concrete structures. *Journal of Engineering Mechanics*, 124(8), 892-900. [https://doi.org/10.1061/\(ASCE\)0733-9399\(1998\)124:8\(892\)](https://doi.org/10.1061/(ASCE)0733-9399(1998)124:8(892))
- Kwak, H. G., & Filippou, F. C. (1990). Finite element analysis of reinforced concrete structures under monotonic loads. *Computers & Structures*, 35(5), 495-508.
- Jankowiak, T., & Łodygowski, T. (2005). Identification of parameters of concrete damage plasticity constitutive model. *Foundations of Civil and Environmental Engineering*, 6, 53-69.

16. Hanif, M. U., Ibrahim, Z., Ghaedi, K., Javanmardi, A., & Rehman, S. K. U. (2018). Finite element simulation of damage in reinforced concrete beams using ABAQUS. *Journal of Civil Engineering, Science and Technology*, 9(1), 10-22.
17. Pazdan, M. (2021). FEM modelling of static behaviour of reinforced concrete beams considering nonlinear concrete behaviour. *Studia Geotechnica et Mechanica*, 43(2), 105-118. <https://doi.org/10.2478/sgem-2021-0012>
18. Abdullah, O. M., Abdulla, A. I., & Alus, W. A. (2024). Numerical assessment of reinforced concrete beams under static loading using ABAQUS. *Samarra Journal of Engineering Science and Research*, 6(1), 45-58.
19. Eligehausen, R., Popov, E. P., & Bertero, V. V. (1983). Local bond stress-slip relationships of deformed bars under generalized excitations. *Earthquake Engineering Research Center, University of California, Berkeley*.
20. Basha, S. H., & Kaushik, S. K. (2016). Flexural behavior of reinforced concrete beams under static loading. *International Journal of Structural Engineering*, 7(2), 134-146.
21. Dassault Systèmes. (2022). *ABAQUS theory guide*. Providence, RI.
22. MacGregor, J. G., & Wight, J. K. (2012). *Reinforced concrete: Mechanics and design* (6th ed.). Pearson Education.
23. Mehta, P. K., & Monteiro, P. J. M. (2014). *Concrete: Microstructure, properties, and materials* (4th ed.). McGraw-Hill Education.
24. Wang, C. K., Salmon, C. G., Pincheira, J. A., & Zárate, B. A. (2018). *Reinforced concrete design* (8th ed.). Wiley.
25. Cook, R. D., Malkus, D. S., Plesha, M. E., & Witt, R. J. (2007). *Concepts and applications of finite element analysis* (4th ed.). Wiley.
26. Crisfield, M. A. (1997). *Non-linear finite element analysis of solids and structures* (Vol. 1). John Wiley & Sons.
27. Dassault Systèmes. (2020). *ABAQUS theory manual*. Providence, RI: Dassault Systèmes Simulia Corp.
28. Yu, T., Teng, J. G., Wong, Y. L., & Dong, S. L. (2010). Finite element modeling of confined concrete—II: Plastic-damage model. *Engineering Structures*, 32(3), 680-691. <https://doi.org/10.1016/j.engstruct.2009.11.013>
29. Kmiecik, P., & Kamiński, M. (2011). Modelling of reinforced concrete structures and composite structures with concrete strength degradation taken into consideration. *Archives of Civil and Mechanical Engineering*, 11(3), 623-636. [https://doi.org/10.1016/S1644-9665\(12\)60105-8](https://doi.org/10.1016/S1644-9665(12)60105-8)
30. Belarbi, A., & Hsu, T. T. C. (1994). Constitutive laws of concrete in tension and reinforcing bars stiffened by concrete. *ACI Structural Journal*, 91(4), 465-474.
31. Torres, L., & Huerta, A. (2007). Numerical modelling of concrete cracking. *Computers & Structures*, 85(9-10), 603-614. <https://doi.org/10.1016/j.compstruc.2006.11.010>

How do I cite this article?

Sai Pavan Bandaru et.al, Finite Element Modeling of Reinforced Concrete Beams Under Static Loading Using Abaqus Software, Excel International Journal of Technology, Engineering and Management, 2026; Volume -13, Issue-2_Page_202-213.

DOI Link: <https://doi.org/10.64971/j.cph.ejtem.v13.i2.22.2026>



This is an open access article under the CC BY-NC-ND license
(<http://creativecommons.org/licenses/by-nc-nd/4.0/>)